Advancing efficiency and mitigating risk: Raman spectroscopy-based analysis of mAb and excipient concentrations throughout downstream

Michelle Nolasco, Nimesh Khadka, Andrew Siemers, Lin Zhang, and Kristina Pleitt,
Thermo Fisher Scientific, 4766 LaGuardia Dr, St. Louis, MO 63134

Abstract

Purpose

Evaluate the feasibility of gathering product and process information through a single, inline measurement thereby increasing process knowledge, minimizing the potential for error, and reducing processing time. Specifically, assess development and application of Raman models for predicting:

1. Monoclonal antibody (mAb) concentration in purified background matrices and clarified harvest for multiple mAbs
2. Formulation excipient concentrations during ultrafiltration/ diafiltration (UF/DF)

Methods

1. Raman models for predicting mAb concentration in purified backgrounds and clarified harvest were developed using a single mAb and tested at bench- and pilot-scale for four mAbs post-harvest, during UF/DF (with traditional and UV-Vis absorbent backgrounds), and during bulk drug substance (BDS) formulation (subset of data shown here); concentration range evaluated ≤ 155 g/L
2. Raman models for predicting L-arginine, L-histidine, and sucrose concentrations were developed and tested at bench- and pilot-scale during UF/DF; concentration ranges evaluated were up to 7 g/L (L-arginine), 4 g/L (L-histidine), and 100 g/L (sucrose)

Results

1. Absolute percent error of the Raman mAb concentration predictions were within 0.1 – 5.8% for all purified matrices at bench- and pilot-scale and within 1.9 – 12.3% for clarified harvest across the mAbs evaluated
2. Absolute percent error of the Raman concentration predictions for L-arginine, L-histidine, and sucrose were within 1.4 – 9.5%, 1.0 – 4.7%, and 3.4 – 10.4%, respectively.

Introduction

Current biopharmaceutical production heavily relies on limited automation along with at-line and offline analytical measurements to control operational parameters and retrospectively inform on process performance. Online and inline process analytical technologies (PAT), such as Raman spectroscopy, can increase process knowledge and understanding, enable automated process control, and reduce process risk[1]. The final UF/DF unit operation can benefit from PAT implementation particularly at high protein concentrations when non-traditional buffer exchange may be observed (e.g., Gibbs-Donnan effect). The specificity of Raman spectroscopy offers solutions for identification, quantification, change monitoring, and additional information about product quality for a broader range of therapeutic proteins[1-3]. Here we show how a generic mAb concentration Raman spectroscopy model along with excipient models can be applied throughout the downstream process to reduce risk, decrease time, and improve process knowledge and understanding through a single, inline measurement.

Materials and methods

Analytical equipment and methods

Raman spectroscopy: Raman spectra for model development and concentration predictions were collected with the MarqMetrix™ All-In-One Process Raman Analyzer (Thermo Scientific) and either a MarqMetrix™ Bioreactor BallProbe™ Sampling Optic (Thermo Scientific) or a MarqMetrix™ FlowCell BallProbe™ (Thermo Scientific). Laser power during acquisition was set to 450 mW with an exposure time of 3000 ms, averaging 3 acquisitions per spectrum (18 s per spectrum). Model predictions were generated with Lykos PAT Software (Thermo Scientific). All spectra were collected at 20 – 22 °C.

Concentration by UV-Vis: Inline protein concentration was determined based on absorbance at 280 nm with scatter correction using the CTech™ FlowVPX® System (Repligen) with a 3 mm flow cell. Offline protein concentration was determined based on triplicate absorbance measurements at 280nm with scatter correction using the CTech™ SoloVPE® System (Repligen).

Analytical protein A chromatography (APAC): mAb concentration was quantified using a POROS™ A 20µm column, 2.1 x 30 mm, 0.1mL analytical affinity column (Thermo Scientific) on a Vanquish UHPLC system (Thermo Scientific).

Carbohydrate profile quantification: Sucrose concentration was quantified using an anion exchange column on an HPLC system. The sample was eluted under basic pH conditions and detected using an Electrochemical Detector.

Development of Raman models

Model training samples

1. *Purified mAb concentration:* Purified mAb1 (IgG1) was concentrated step-wise via a UF/DF process with the MarqMetrix™ FlowCell BallProbe™ inline. Twelve samples (0 – 150 mg/mL) in various buffer backgrounds were generated for model training. An example of the spectra is shown in Figure 1A.
2. *Clarified harvest mAb concentration:* Two clarified harvest pools containing mAb1 and mAb4 (IgG1) were concentrated by a 10 kDa centrifugal filter and diluted with filtrate to generate 24 training samples, up to. 9.4 g/L. An additional twelve training samples were generated by spiking purified, concentrated mAb1 into protein A chromatography load flowthrough.
3. *Excipient concentrations:* Twelve solutions containing L-arginine (Thermo Scientific), L-histidine (Pfanstiehl), and sucrose (J.T. Baker) were prepared based on a Uniform Design space. The component concentrations [up to 45 g/L (258 mM) for L-arginine, 14 g/L (67 mM) for L-histidine, and 200 g/L (584 mM) for sucrose] were selected based on ranges for high protein concentration formulations[4]. Additional samples from the step-wise UF/DF experiment were added to the training data set. An example of the spectra is shown in Figure 1B.

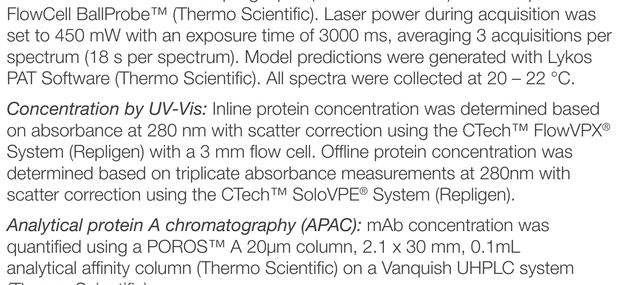

Figure 1. Example Raman spectra from model training for A) protein concentration and B) excipients (L-arginine, L-histidine, and sucrose).

Model development

1. *Purified mAb concentration:* A Partial Least Squares (PLS) regression model was developed for predicting mAb concentration using SOLO Eigenvector software. Each spectrum was preprocessed using normalization to water band and followed by application of Savitzky-Golay filter (1st derivative; polynomial order=2; window width=13) and mean centering. The PLS model was developed using only a specific region of the spectra to enable model application across different mAbs and processes. A leave-out-one cross validation (CV) strategy was adopted for internal validation of the model. The root mean square error of CV (RMSECV) was used as criteria to select the number of latent variables for the PLS model.
2. *Clarified harvest mAb concentration:* The PLS model to quantify mAb in clarified harvest was developed using the spectral region of 800 to 3250 cm^{-1}. The training data spanned the concentration range of 0 to 9 g/L. Each spectrum was preprocessed using normalization to water band and followed by application of Savitzky-Golay filter (1st derivative; polynomial order=2; window width=13) and mean centering. The PLS model was internally validated using K-5 fold cross validation. Based on the RMSECV, 5 latent variables PLS was selected. The validity of the model was assessed using the variable importance in projection plot, specificity plot, and permutation test.
3. *Excipient concentrations:* Individual PLS models for L-histidine, L-arginine, and sucrose were built following the methods as described for purified mAb concentration.

Model verification

1. *Purified mAb concentration:* The predictive performance and generalizability of the model was assessed by applying the model to the Raman spectra independently collected for four mAbs with the Raman FlowCell.
2. *Clarified harvest mAb concentration:* The model performance was assessed with the Raman FlowCell for two clarified harvest. Samples were concentrated using centrifugal filters to test a range of concentrations.
3. *Excipient concentrations:* Seven independent solutions with varying levels of L-arginine, L-histidine, and sucrose were used for model verification with spectra collected using the Raman FlowCell. Spectra were collected with three different instruments to assess instrument variability.

Bioprocess workflow application

Harvest clarification: CHO cells expressing mAb were cultured in a 500 L DynaDrive Single-Use Bioreactor (Thermo Scientific) via a fed-batch process. The cultures were clarified using a DynaSpin Single-Use Centrifuge (Thermo Scientific) followed by Millistak+® B1HC Pod depth filters (Millipore Sigma). Four different cultures were produced; three contained IgG1 and one contained an IgG4. To test a range of concentrations, clarified harvest was concentrated using 10 kDa centrifugal filters. The Raman mAb concentration predictions shown here are from cultures containing IgG1.

UF/DF: The mAbs were purified from the clarified harvest (above) using a two-chromatography step platform process. The final UF/DF was performed at bench- (100 cm^2) and pilot-scale (2.5 m^2) using TangenX ProStream 50 kDa cassettes (Repligen). Membrane loadings were ≤ 550 g/m^2. The feed flow rate was 300 LMH and transmembrane pressure was controlled at ≤ 20 psid. The MarqMetrix™ FlowCell BallProbe™ was placed inline on the feed side for all experiments, and the MarqMetrix™ Bioreactor BallProbe™ was connected to the retentate vessel for pilot-scale experiments. Starting mAb concentrations ranged from 2 – 12 mg/mL (based on UV-Vis). The pools were concentrated to 20 – 50 mg/mL prior to DF. DF occurred with the mAb-specific formulations (two IgG1 and one IgG4) or a buffer containing a UV-absorbing amino acid (one IgG1) for 7 diavolumes. After DF the pools were concentrated to 85 – 156 mg/mL. The UF/DF system was drained (primary recovery) and flushed with 1.5x system hold-up volume with DF buffer (secondary recovery).

Formulation: The primary recovery product pools (above) were diluted with the secondary recovery (above) to 54 – 83 mg/mL prior to formulation with the appropriate formulation buffer containing polysorbate 80.

Results

Raman mAb concentration models

Figure 2A shows the cross validated results of the PLS model developed for mAb in purified matrices. The RMSECV did not improve by adding additional latent variables thus the three latent variable PLS model was selected. The RMSECV of 0.677 mg/mL and the R^2 of CV ~1 (note: software does not report beyond three decimal places) indicate good predictive performance and fit to the training data, respectively. Similarly, Figure 2B shows the PLS regression model with five latent variables for clarified harvest samples containing mAb with RMSECV of 0.159 mg/mL and the R^2 of CV 0.997.

mAb concentration prediction: UF/DF

Performance of the mAb concentration model for purified matrices was tested during UF/DF operation. Figure 3 shows an example of the mAb concentration prediction for mAb3 during a pilot-scale UF/DF operation. As the system was equilibrated, the model reported no mAb concentration. As the product pool was introduced to the system and concentrated, the model predicted a steady increase in concentration from 1.0 to 44 mg/mL.

Throughout DF, the concentration prediction remained consistent. UF2 had a rapid increase in concentration followed by a more gradual change as the final concentration target was approached. The variable rate of change was a result of operational variation. Similar performance was observed for other the mAbs and at bench-scale.

Figure 4 compares the Raman predicted mAb concentration values and inline UV-Vis mAb concentration values for a UF/DF process where mAb1 is exchanged into a matrix containing a UV-absorbing amino acid. During UF1, both methods indicate similar concentrations (note: the stable concentration value of 20 mg/mL during UF1 is a result of a process pause). During DF, the Raman prediction remains steady while the inline UV-Vis measurement increases to 73 mg/mL due to the addition of the UV-absorbing amino acid to the product pool. Both measurements show similar rates of change during UF2, but the reported end concentration values are different (UV-Vis: 192 mg/mL and Raman: 156 mg/mL).

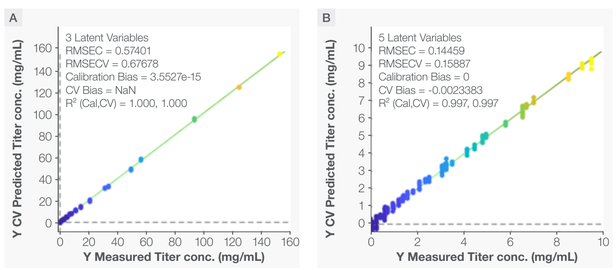

Figure 2. Model fit results for mAb concentration in A) purified pools and B) clarified harvest.

Scale	mAb	Predicted concentration (mg/mL) [% error to offline UV-Vis or APAC]		
		End of UF1	End of DF	End of UF2
Bench	mAb1	33.8 [-1.1%]	31.3 [0.1%]	133.2 [0.1%]
	mAb1 [a]	23.4 [4.6%]	30.7 [-0.7%] [a]	155.9 [-0.5%] [a]
	mAb2	42.1 [-3.1%]	35.0 [-3.8%]	94.5 [-2.5%]
Pilot	mAb1	38.1 [2.2%]	40.5 [4.1%]	85.3 [5.8%]
	mAb3	44.2 [3.9%]	41.9 [2.8%]	103.3 [-1.6%]

Note: [a] Experiment used a DF buffer containing a UV-absorbing amino acid. Reference measurement was APAC (average of 5 dilutions). All other points compared to UV-Vis measurements.

Table 1. Predicted mAb concentration and percent error to offline UV-Vis or APAC measurement for bench- and pilot-scale ultrafiltration (UF)/ diafiltration (DF) of different mAbs.

mAb	Predicted concentration (mg/mL) [% error to offline UV-Vis]	
	Post-UFDF dilution	Formulated BDS
mAb1	53.6 [3.3%]	50.4 [5.1%]
mAb4	83.4 [-1.5%]	75.7 [0.0%]

Table 2. Raman mAb concentration prediction and percent error to offline UV-Vis measurement for post-UF/DF recovery and formulation

mAb	Predicted concentration (mg/mL) [% error to APAC]	
	Low	Moderate
mAb1	2.0 [8.9%]	4.3 [-4.4%]
mAb4	2.3 [12.3%]	4.6 [4.5%]

Table 3. Raman mAb concentration prediction and percent error to analytical protein A chromatography (APAC) in clarified harvest for mAb1 and mAb4.

Scale	Predicted concentration (mg/mL) [%error to formulation concentration]		
	L-arginine	L-histidine	Sucrose
Bench	7.1 [1.4%]	4.1 [1.0%]	95.6 [3.4%]
Pilot	6.0 [9.5%]	4.4 [4.7%]	102.5 [10.4%]

Table 4. Raman excipient concentration prediction and percent error to formulation concentration at the end of bench- and pilot-scale DF of mAb1.

Table 1 shows the predicted concentration at the end of UF1, DF, and UF2 for different mAbs at bench- and pilot-scale along with the percent error compared to the offline UV-Vis value or APAC (for matrices containing the UV-absorbing amino acid). The target concentrations varied depending on the process and the availability of material. However, model prediction performance was consistent between mAbs and process scales. In all cases, the absolute error was less than 6%.

mAb concentration prediction: BDS formulation

After UF/DF the primary recovery pool was diluted with the secondary recovery pool to within 10% of the final target mAb concentration based on the Raman model mAb concentration prediction. The pool was then spiked with formulation buffer containing polysorbate 80. Table 2 lists the predicted mAb concentration values after the dilution and formulation for mAb1 and mAb4. The percent error compared to offline UV-Vis measurement were within 5% indicating accurate model prediction performance.

mAb concentration prediction: clarified harvest

Prediction of mAb quantification in clarified harvest was evaluated with two cultures. One clarified harvest pool had standard levels of process-related impurities (mAb1) and the other had low levels (mAb4). The predictions and associated percent error to APAC are shown in Table 3. The model was accurate at moderate mAb concentration levels (error within ± 5%), but error increased at lower mAb concentrations. Additionally, lower concentration predictions had more noise in the data set.

Raman excipient concentration models

Figure 5A - C respectively shows the performance of the L-arginine, L-histidine, and sucrose PLS models when applied to independent test samples using three different instruments without applying any transfer function. The model statistics for training and prediction is shown as inset for each plot. The RMSECV and R^2 values for the three models indicate good predictive performance and fit to the training data, respectively. The low root mean square error of prediction (RMSEP), prediction bias, and R^2 (prediction) across all three instruments indicate excellent prediction of model and minimum inter-instrument variance that allows accurate model transferability.

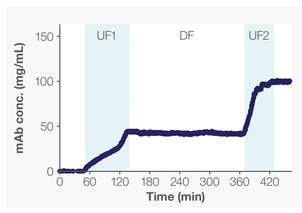

Figure 3. Raman concentration prediction of mAb3 versus time during pilot-scale ultrafiltration (UF)/ diafiltration (DF).

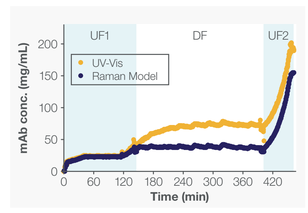

Figure 4. mAb1 concentration in a background matrix with UV-Vis absorbance versus time during bench-scale ultrafiltration (UF)/ diafiltration (DF); Inline UV-Vis based concentration in yellow, Raman predicted concentration in blue.

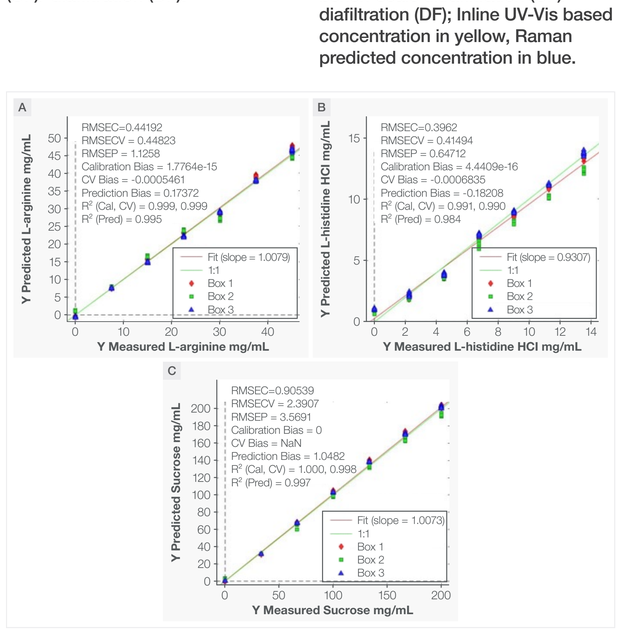

Figure 5. Model fit results for A) L-arginine, B) L-histidine, and C) sucrose.

Excipient concentration prediction: UF/DF

Excipient concentration predictions were monitored during UF/DF at bench- and pilot-scale to evaluate the feasibility of using Raman as an in-process check for proper formulation of the product pool. Figure 6A - C show the predictions for L-arginine, L-histidine, and sucrose, respectively. Throughout DF, the prediction for each excipient increases to the concentration of the DF buffer. During UF2, the predicted sucrose concentration is observed to decrease by > 10%. The decreasing sucrose trend was corroborated via offline HPLC analysis.

Table 4 lists the predicted excipient concentrations at the end of DF for mAb1 at bench- and pilot-scale. Error compared to the buffer concentration was < 4% for all excipients. Higher error occurred at the pilot-scale.

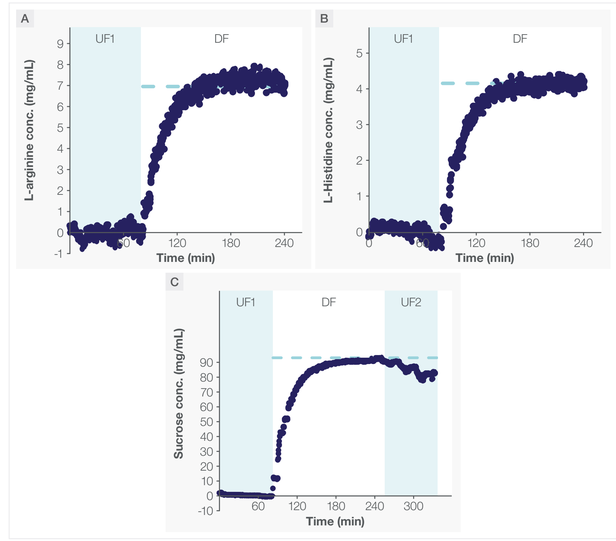

Figure 6. Raman concentration (conc.) predictions versus time during bench-scale UF/DF of mAb1 for A) L-arginine, B) L-histidine, and C) sucrose; target end conc. shown with light blue dashed line.

Discussion and conclusions

The use of Raman spectroscopy as a novel technique for mAb concentration measurement offers significant advantages over traditional methods such as UV-Vis, particularly in cases where the background matrix exhibits UV absorbance. By providing real-time, accurate prediction of mAb concentration and eliminating the need for offline assays, Raman spectroscopy enhances the efficiency of biomanufacturing processes and reduces process risk.

The performance of the Raman mAb concentration model for purified mAb was successfully demonstrated for both bench-scale and pilot-scale UF/DF and formulation processes, encompassing a variety of mAbs and buffer backgrounds (three traditional and one UV-absorbing). The model had a high level of accuracy, with measurements falling within less than 6% of reference values. Notably, this accuracy was maintained across different IgG subclasses (IgG1 and IgG4). The breadth of application demonstrated by the model, along with its ability to maintain accuracy, indicates strong generalizability. However, future evaluations should explore the model's performance with other IgG subclasses, such as IgG2, and assess its applicability to a wider concentration range.

In addition to the purified mAb concentration model, a separate model was developed for clarified harvest backgrounds. This model's applicability was successfully demonstrated for two mAbs of the IgG1 subclass, originating from different production cultures and containing varying levels of process-related impurities. The concentrations tested exhibited good applicability for fed-batch production, although further refinement is necessary to improve accuracy at lower concentrations, particularly relevant for perfusion production. Additionally, the model should be tested with higher mAb concentrations and evaluated for different IgG subclasses.

The formulation excipient models, specifically L-histidine, L-arginine, and sucrose, demonstrated accuracy within 10% of expected values. Notably, the sucrose model accurately predicted a decrease in concentration during the UF2 step, thereby identifying common concerns related to volume exclusion effects and imbalances of charged ions at higher concentrations of mAb. These predictions enable real-time detection and correction of these phenomena, providing valuable insights for process optimization. To refine the amino acid excipient models further, a deeper understanding of the impact of protein signals in the spectra is required to achieve more accurate quantification at higher mAb concentrations.

Implementing Raman spectroscopy as PAT for real-time mAb and excipient concentration measurements offers significant potential for time savings and efficiency improvements. By implementing inline mAb concentration measurement, downstream processing time could be reduced by an estimated 3-5% per batch, leading to increased throughput for biomanufacturers. This reduction in processing time could enable the manufacture of an additional two batches per year per suite, assuming an average downstream cadence of 7 days and minimum of 80% suite utilization.

Furthermore, real-time monitoring capabilities provided by Raman spectroscopy enable immediate detection of concentration deviations, allowing for timely adjustments and interventions. This not only minimizes resources required for deviation management but also mitigates potential product losses. By removing operator interaction with the process and enabling data-driven decision making, the risk associated with the manufacturing process is significantly reduced.

The demonstrated concentration model's ability to work in various background matrices expands formulation options without compromising manufacturability. Additionally, the model's generalizability to different mAbs within the same subclass and across different subclasses has the potential to reduce analytical method transfer resource requirements.

Moreover, the Raman models enable continuous processing by providing real-time, inline concentration values throughout the downstream process. This information can be utilized for feedback control, from loading clarified harvest onto protein A chromatography columns to achieving the target concentration of purified product. Overall, the incorporation of Raman spectroscopy as a PAT tool enhances process control, efficiency, and product quality in biomanufacturing.

References

1. Esmonde-White, K. A., Cuellar, M., & Lewis, I. R. (2022). The role of Raman spectroscopy in biopharmaceuticals from development to manufacturing. Analytical and Bioanalytical Chemistry, 1-23.
2. Goldrick, S., Umprecht, A., Tang, A., Zakrzewski, R., Cheeks, M., Turner, R., . . . Spencer, C. (2020). High-throughput Raman spectroscopy combined with innovate data analysis workflow to enhance biopharmaceutical process development. Processes, 8(9), 1179.
3. Rolinger, L., Ruedt, M., & Hubbuch, J. (2020). A critical review of recent trends, and a future perspective of optical spectroscopy as PAT in biopharmaceutical downstream processing. Analytical and Bioanalytical Chemistry, 412, 2047-2064.
4. Wang, S. S., Yan, Y., & Ho, K. (2021). US FDA-approved therapeutic antibodies with high-concentration formulation: summaries and perspectives. Antibody therapeutics, 4(4), 262-272.

Learn more at **thermofisher.com/marqmetrixAIO**